AGU PUBLICATIONS

JGR

Journal of Geophysical Research: Biogeosciences

RESEARCH ARTICLE

10.1002/2017JG004046

Key Points:

- Woody encroachment of grasslands is occurring globally
- A low-dimensional model is used to examine fire frequency, precipitation frequency, and magnitude on the rate of woody encroachment
- Lyapunov exponents show that the rate of woody encroachment is dominated by the fire frequency

Correspondence to:
N. A. Brunsell,
brunsell@ku.edu

Citation:
Brunsell, N. A., Van Vleck, E. S., Nosshi, M., Ratajczak, Z., & Nippert, J. B. (2017). Assessing the roles of fire frequency and precipitation in determining woody plant expansion in central U.S. grasslands. *Journal of Geophysical Research: Biogeosciences*, *122*, 2683–2698. https://doi.org/10.1002/2017JG004046

Received 14 JUL 2017
Accepted 25 SEP 2017
Accepted article online 5 OCT 2017
Published online 24 OCT 2017

Assessing the Roles of Fire Frequency and Precipitation in Determining Woody Plant Expansion in Central U.S. Grasslands

N. A. Brunsell[1], E. S. Van Vleck[2], M. Nosshi[1], Z. Ratajczak[3], and J. B. Nippert[4]

[1]Department of Geography and Atmospheric Science, University of Kansas, Lawrence, KS, USA, [2]Department of Mathematics, University of Kansas, Lawrence, KS, USA, [3]Department of Zoology, University of Wisconsin, Madison, WI, USA, [4]Division of Biology, Kansas State University, Manhattan, KS, USA

Abstract Woody plant expansion into grasslands and savannas is occurring and accelerating worldwide and often impacts ecosystem processes. Understanding and predicting the environmental and ecological impacts of encroachment has led to a variety of methodologies for assessing its onset, transition, and stability, generally relying on dynamical systems approaches. Here we continue this general line of investigation to facilitate the understanding of the roles of precipitation frequency and intensity and fire frequency on the conversion of grasslands to woody-dominated systems focusing on the central United States. A low-dimensional model with stochastic precipitation and fire disturbance is introduced to examine the complex interactions between precipitation and fire as mechanisms that may suppress or facilitate increases in woody cover. By using Lyapunov exponents, we are able to ascertain the relative control exerted on woody encroachment through these mechanisms. Our results indicate that precipitation frequency is a more important control on woody encroachment than the intensity of individual precipitation events. Fire, however, exerts a much more dominant impact on the limitation of encroachment over the range of precipitation variability considered here. These results indicate that fire management may be an effective strategy to slow the onset of woody species into grasslands. While climate change might predict a reduced potential for woody encroachment in the near future, these results indicate a reduction in woody fraction may be unlikely when considering anthropogenic fire suppression.

1. Introduction

The expansion of woody plants into grasslands is pervasive and increasing around the globe (Eldridge & Soliveres, 2014; Myers-Smith et al., 2011; Stevens et al., 2016). Woody and grass species respond to environmental drivers such as precipitation frequency and magnitude, fire frequency and intensity, grazing pressure, and local site characteristics such as soil texture, and access to deep water sources (Archer et al., 1995; Bond, 2008; Scholes & Archer, 1997). These species level responses determine their relative contributions to the global incursion of woody species on grasslands. There is increasing pressure to understand how changes in these environmental factors are impacting this dramatic shift in vegetation composition across the globe and the potential consequences of this transformation (Van Auken, 2000).

Consensus has traditionally coalesced around mean annual precipitation (MAP) as an overarching factor determining woody plant dynamics at the continental- (Barger et al., 2011; Lehmann et al., 2014; Sankaran et al., 2005) as well as the global scale (Eldridge et al., 2011; Staver et al., 2011) due to the competitive advantage of woody plants in accessing the increased amount of water deeper in the soil and as superior competitors for light when water-limitation declines. There is strong evidence that the intensity of precipitation is a primary control on woody fraction (Kulmatiski & Beard, 2013; Xu et al., 2015). This is supportive of the hypothesis that increased precipitation results in increased deep water infiltration and availability and thus favors woody species (Walker & Noy-Meir, 1982). However, in some cases, this is not observed due to an increased transpiration from the grass species resulting in a decrease in deep water availability (February et al., 2013; Holdo & Nippert, 2015), highlighting the complex nature of interactions between different species' response strategies to stochastic forcing.

The temporal distribution of precipitation is governed by both the intensity of individual events (α) and the frequency of those events (λ). This can result in regions with similar mean annual precipitation (MAP) having markedly different woody cover (Good & Caylor, 2011; Staver et al., 2011). Therefore, to understand the potential woody cover requires an understanding of intraannual rainfall patterns, not just annual averages (Good & Caylor, 2011; Knapp & Smith, 2001). Nevertheless, it has been well noted that the climate hypothesis, or any single factor explanation for that matter, is insufficient in explaining why major biomes such as C_4 grasslands and savannas exist when they have sufficient MAP to support a closed canopy of trees (Bond, 2008).

Within this overarching water limitation on potential woody cover, other factors such as land use, soil, and disturbances are thought of as secondary and relatively localized drivers of potential woody cover. A look at the global pattern of woody encroachment is consistent with this framework, being predominantly abrupt, or discontinuous in form (D'Odorico et al., 2012; Staver et al., 2011). This is particularly evident toward the wetter end of the precipitation gradient (1,000 mm to 2,500 mm annual totals), with less than extreme seasonality ($\leqslant$7 month dry season), where alternative stable states, between forest and savanna, are maintained by fire and where humans have greatly altered fire regimes (Eldridge et al., 2011; Nowacki & Abrams, 2008; Staver et al., 2011).

From both an ecological and managerial perspective there is interest in understanding how environmental drivers interact with the woody cover to facilitate future woody encroachment (Twidwell, Rogers et al., 2013). This information is critical, because accumulating evidence suggests that woody plants can incite positive feedbacks that make reversing woody plant expansion difficult, because water limitation of woody plants and fire intensity decreases with increasing woody cover (Ratajczak, Nippert, & Ocheltree, 2014; Ratajczak, Nippert, Briggs, et al., 2014). Woody species are known to impact the water use at a site (Brunsell et al., 2014; Honda & Durigan, 2016; Nippert et al., 2013), the overall ecosystem scale carbon and water cycling (Knapp et al., 2008; Logan & Brunsell, 2015), and ultimately, the diversity of the vegetative community (Eldridge et al., 2011). These local scale vegetation-climate interactions have also been linked to regional changes in response to global climate change (Brovkin et al., 1998; Claussen et al., 1999; Dekker et al., 2007).

The factors controlling the fractional coverage of woody species are complex (Bond, 2008). The stability of woody tree fraction is governed by a multitude of nonlinearly interacting factors such as climate, fire, and grazing. Koerner and Collins (2014) investigated the relative contributions of grazing, drought, and fire on mesic grasslands in North America and South Africa, and found that even with different evolutionary histories, both sites responded similar to changes in grazing, drought, and fire with respect to grassland productivity. Fuhlendorf et al. (2008) discuss the complications of fire and grazing combinations for woody species expansion and concluded that U.S. grasslands required fire to be maintained. While grazing may be an important factor globally, there is also evidence that at the Konza Prairie, the impacts of grazing are less important (Briggs et al., 2005; Ratajczak, Nippert, Briggs, et al., 2014). Precipitation patterns were important primarily for ecosystems nearing transitions between woody and grass species. Under high rainfall regimes, they conclude that grazing reduces fuel loads required to burn woody species, and that under grazed conditions, the fire frequency required to maintain a grassland increased from 1 burn every 10 years to approximately 1 burn every 2–3 years (Fuhlendorf et al., 2008). In addition to the changing climate, fire, and grazing environment, there is also the potential that increases in atmospheric CO_2 may benefit the increase in woody fraction by decreasing water limitation (Schlaepfer et al., 2017).

The potential for self-reinforcing feedbacks has led to an increased focus on the role of fire as a control factor to encourage or slowdown the process of woody encroachment (Fuhlendorf & Engle, 2004; Ratajczak, Nippert, Briggs, et al., 2014; Twidwell, Fuhlendorf, et al., 2013). Although fire is important, it may be a secondary driver following annual precipitation in determining woody fraction, and therefore, the ongoing debate on fire suppression might be trivial from a managerial standpoint (Higgins et al., 2010; Sankaran et al., 2005). Yet a growing number of experiments suggest that the ability of fire to reduce woody biomass declines greatly as woody fraction increases (Ratajczak, Nippert, Briggs, et al., 2014; Wonkka et al., 2016), implying that increasing fire frequency might only be an effective control mechanism in regions only beginning to experience woody plant expansion, even if water limitation of woody plants increases.

Understanding and predicting the conversion of grasslands and savannas has led to a variety of methodologies for assessing the onset, transition, and stability of encroachment, generally relying on dynamical systems approaches (D'Odorico et al., 2012; Ratajczak, Nippert, Briggs, et al., 2014). An analytical technique that may be useful in assessing the complex, nonlinear interactions of the increase in woody fraction is the use

of Lyapunov exponents. As an indicator of chaos (i.e., sensitivity to the initial state) and a measure of the relative sensitivity of parameterized systems, the largest Lyapunov exponent has been employed successfully in different areas of biology and ecology, in particular to assess the rate of transition between on state and another (Cushing et al., 2002). For example, Lyapunov exponents are indicative of the exponential rate of change of a dynamical system either away or toward a particular state of the system, for example, a grass or woody state. Therefore, a positive exponent illustrates an exponential rate away from the current state, for example, an unstable state and a transition from the unstable state to a stable state. While a negative exponent indicates a trajectory toward the initial state, that is, that state is stable. Therefore, if a given precipitation environment results in a negative (positive) Lyapunov exponent for woody fraction, this would indicate that the particular rainfall regime is stable (unstable) for the expansion of woody species. Dakos et al. (2009) investigated the interannual variability in species composition, and seasonal forcing increased the occurrence of chaos (i.e., the internal variance of the plankton population). By employing Lyapunov exponents, they showed how the amplitude of seasonal forcing affected the occurrence of chaos, the interannual variability, that is not explained by the variance of the forcing variables (e.g., weather) in the populations considered. Graham et al. (2007) employed Lyapunov exponents to investigate biological nitrification and showed that chaotic behavior is central to stability in nitrification. They showed that two bacteria guilds were sensitive to initial conditions, but Lyapunov exponents were able to characterize a fragile mutualism that showed the variance in the two populations was susceptible to instability in the other populations. Molz and Faybishenko (2013) provide background and recent developments in soil-plant-atmosphere systems and their analysis using nonlinear dynamics techniques and suggest the possibility that chaotic dynamics as characterized by a positive Lyapunov exponent is inherent for sustainability of natural ecological and agricultural systems.

The objective of this work is to examine the nonlinear interactions governing the expansion of woody species in grasslands by focusing on the roles of fire and precipitation, and their relative roles in controlling the amount of woody encroachment in the central United States grasslands. Here we continue the application of dynamical systems techniques to facilitate the understanding of the roles of precipitation and fire regimes on the conversion of grasslands and assess overall stability of woody fraction under a prescribed fire and precipitation scenario. By using Lyapunov exponents, we are attempting to ascertain the relative control exerted on woody encroachment by environmental drivers (precipitation) and fire disturbance. This will ultimately inform our understanding of both the underlying dynamics in these environments as well as offer insight into more effective management strategies.

2. Methods

2.1. Field Data

The Konza Prairie Biological Station (KPBS) is used as a site case study in this analysis. The Konza Prairie is located south of the city of Manhattan in north-central Kansas. The site consists of 3,847 ha of native tallgrass prairie on the western edge of the historic range (Figure 1). The site experiences a midcontinental climate with an annual precipitation of 844 mm, approximately 75% of which occurs during the growing season (April – September). The site is managed at the watershed scale, with replicates of various burn frequency and grazing regimes. For the present work, three ungrazed watersheds are considered: an annually burned watershed (watershed 1-D, with Ameriflux site US-KON), a 4 year burn (watershed 4B, Ameriflux site US-KFB), and a 20 year burn (watershed 20B). Dominant grass species are perennial C_4 grass species (*Andropogon gerardii*, *Panicum virgatum*, *Schizachyrium scoparium*, and *Sorghastrum nutans*). A recent nonlinear growth of dogwood (*Cornus drummondii*) has been observed at KFB (Ratajczak et al., 2011). The 20B watershed is dominated by a mix of *Juniperus virginiana*, *Cornus drummondii*, *Gleditsia triacanthos*, and the herbaceous plants. Soils vary across the site with the upland regions consisting of shallow, surficial Florence limestone bedrock (~0.5 m), while soils in the lowland regions consist of silty-clay loams (Tully soils) and can extend to approximately a 2 m depth (Schimel et al., 1991). Precipitation data for the period of 1983 – 2015 were collected at the Konza Prairie Headquarters building located within 5 km of each watershed.

Fire occurrence and woody fraction data for the period were collected separately in each of the three watersheds. The woody fraction data are derived from 4 year, 50 m long vegetation composition transects for each of the three fire frequencies (annual [watershed 1D, US-KON], 4 year [watershed 4B, US-KFB], and 20 year [watershed 20B] returns). Each transect is composed of five equally spaced 10 m^2 circular plots, for a total of 20 plots per treatment. The approximate cover of all species within these plots has been recorded each year since 1983 using a cover scale. We report the aggregate cover of all woody species capable of developing

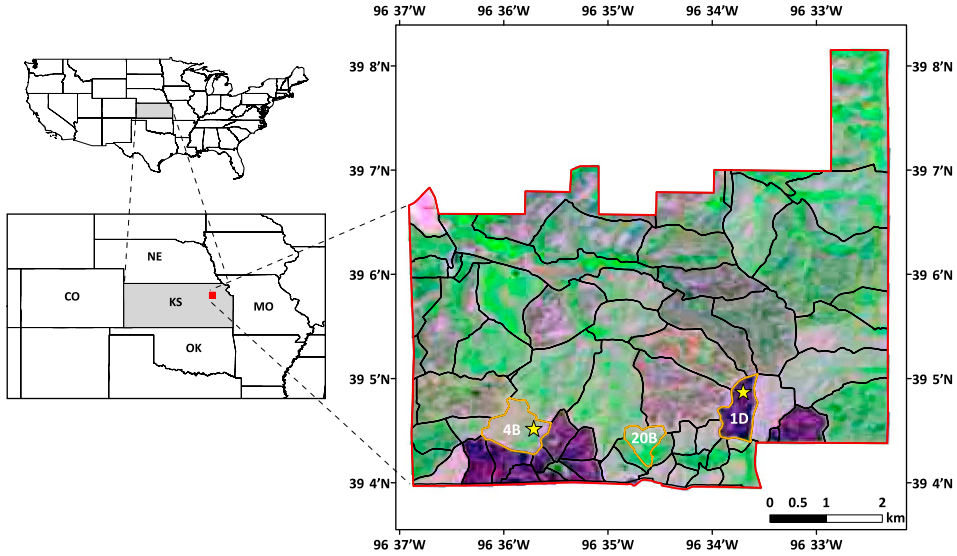

Figure 1. Map illustrating the location of the Konza Prairie Biological Station. The colors represent a natural color band composition where red (band 6), green (band 5), and blue (band 4) for the Landsat scene acquired on 10 May 2016. The 1 year watershed (1D), 4 year burn (4B), and 20 year burn (20B) watersheds used in this analysis are highlighted. In addition, the locations of the eddy covariance stations in 1D (US-KON) and 4B (US-KFB) are indicated.

a canopy taller than the dominant grasses (~1.5 m), which are tall shrubs and trees. In some instances, the aggregate cover of woody species exceeded 100%, due to the presence of overlapping shrub canopies. In such plots, the woody fraction is considered to be 100%. With the exception of coercing plots with >100% woody cover, all fractions are identical to Ratajczak, Nippert and Ocheltree (2014).

There are two Ameriflux eddy covariance towers at the Konza Prairie. Data from 2008 to 2014 were used from the annually burned site (US-KON) and the 4 year burn site (US-KFB) located approximately 1 mile apart from one another. There is no eddy covariance tower on the 20 year burn watershed used in this analysis (20B). Unfortunately, 2012 data from the KFB site were unavailable. Data from the site is collected at the sites 3 m above the surface. Three-dimensional wind components, temperature, humidity, and carbon dioxide concentration are collected at 20 Hz using a triaxial sonic anemometer (CSAT-3, Campbell Scientific, Logan UT, USA) and a Li-Cor infrared gas analyzer (LI-7500, Li-Cor, Lincoln, NE, USA). Half hour data are processed according to Ameriflux standards and are described in Brunsell et al. (2014), and missing values of the fluxes are gap filled following Reichstein et al. (2005).

2.2. Modeling Temporal Dynamics of Woody Encroachment

Building on our previous efforts (Petrie & Brunsell, 2011; Petrie et al., 2011), we have adopted a low-dimensional modeling framework based primarily on the assumption of water limitation governing the water and carbon cycling in many grassland ecosystems. This model is an extension of the approach utilized in Porporato (2003). We extend the model previously presented to include a deeper soil moisture layer, competition between woody and grass species, and a stochastic fire model.

The model is forced with a simple stochastic precipitation scheme in which the frequency (λ) and intensity (α) of precipitation events within the year are given as inputs. The timing of precipitation is generated as a Poisson process with parameter λ, and the magnitude of precipitation events is generated as an exponential random variable with parameter α. The precipitation parameters are determined at the annual scale, and thus, no seasonality of rainfall is incorporated in the model.

The daily time series of precipitation represents the only water source to the surface. To incorporate woody species, which have greater access to deeper soil water than grasses, we have expanded the model to a two-layer soil model. The soil moisture in the top layer is modeled as

$$\frac{d\theta_1}{dt} = P - L_1 - f_s E_s - f_g T_g - f_w \epsilon_w T_w, \quad (1)$$

where P is the daily precipitation, L_1 is the drainage to the deeper soil layer, E_s is the bare soil evaporation, T is the species specific transpiration (grass and woody) that is scaled by their relative fraction (f), and ϵ_w is the fraction of water withdraw from the upper soil layer by the woody vegetation (set to 0.15). While the actual soil depths at the Konza Prairie range from tens of centimeters to several meters, for the simulation purposes, we assume that the top soil depth is 50 cm and the overall depth is 2 m (deep layer is 1.5 m thick).

Only woody plants have transpiration from the bottom layer, so the soil moisture balance for the deeper layer is

$$\frac{d\theta_2}{dt} = L_1 - f_w(1-\epsilon_w)T_w - Q_l, \tag{2}$$

where Q_l is drainage from the second layer.

Drainage from the top to the lower soil layer is

$$L_1 = -K_{s,\text{eff}} + K_{s,\text{eff}}\frac{d\Psi}{d\theta}\left(\frac{\theta-\theta_d}{z_r + (z_{r,d}-z_r)/2 - (z_r)/2}\right), \tag{3}$$

where the effective hydraulic conductivity ($K_{s,\text{eff}}$) of each soil layer is estimated:

$$K_{s,\text{eff}} = K_s\left(\frac{\theta-\theta_d}{\theta_{fc}-\theta_h}\right)^{(2b+3)}, \tag{4}$$

where K_s is the saturated hydraulic conductivity of the layer, θ is the soil moisture value in that layer, θ_d is wilting point, θ_{fc} is the field capacity value, and θ_h is the hygroscopic point. The values chosen for the simulations are representative of the Konza Prairie soils (Petrie & Brunsell, 2011).

The evaporative losses from the surface are represented by a maximum function that encompasses an annual cycle peaking in the summer and with a minimum in the winter. The maximum daily evapotranspiration (E_{max}) is estimated as

$$E_{\text{max}} = E_0(1 + \delta\sin((\omega_t J) + \phi_{\text{et}})), \tag{5}$$

where the value of the potential E_{max} for day of year (J) oscillates around E_0, δ is the ratio of the amplitude to $E_{\text{max},0}$, ϕ_{et} is a phase shift, and ω_t is the frequency. For these simulations, the maximum annual value of E_{max} is 6 mm/d representative of the Konza Prairie (Petrie & Brunsell, 2011).

The actual bare soil evaporation (E) is determined from the E_{max} with a linear reduction based on soil moisture:

$$E = \begin{cases} 0, & \text{if } 0 < \theta \le \theta_h \\ E_w\frac{(\theta-\theta_h)}{(\theta_w-\theta_h)}, & \text{if } \theta_h < \theta \le \theta_w \\ E_w + (E_{\text{max}} - E_w)\frac{(\theta-\theta_h)}{(\theta_w-\theta_h)}, & \text{if } \theta_w < \theta \le \theta_* \\ E_{\text{max}}, & \text{if } \theta > \theta_*, \end{cases} \tag{6}$$

where θ_d is wilting point, θ_{fc} is the field capacity value, and θ_h is the hygroscopic point.

Woody species and grasses both have an annual phenological cycle based on the day of year. Onset is modeled as a linear increase at the beginning of the growing season, and senescence is a linear decrease at the end of the growing season based on beginning and ending dates (g_s, g_d); between those dates, the growth reaches maturity on (g_m) and begins senescence on g_b. In the current simulations, these values were chosen to be consistent with the eddy covariance observations and were set to g_s = 90 and g_d = 292 for the grasses and for the woody component g_s = 80 and g_d = 292. Both species mature over a 30 day period and senesce over a 20 day period.

Carbon assimilation is determined in a similar manner as the transpiration with the addition of the species specific annual phenological curve described above. While there is no explicit temperature dependence incorporated into the model, the daily value of A_{max} is determined from the E_{max} with a prescribed seasonality with a maximum in the middle of the year. This E_{max} and the species level water use efficiency (WUE) are used to calculate the maximum amount of daily assimilation as

$$A_{\text{max}} = \frac{E_{\text{max}}}{18.016}\text{WUE}. \tag{7}$$

In the present simulations, the WUE is based on eddy covariance observations (Brunsell et al., 2014), and for the grass it is 0.26 and for the woody species it is 0.35. Note that while the grass has a higher WUE at the leaf scale, when scaled to the eddy covariance footprint the woody species have a higher WUE (Brunsell et al., 2014).

The actual daily value of the assimilation is reduced with increasing water stress:

$$A = \begin{cases} 0, & \text{if } 0 < \theta \le \theta_w \\ A_{\max}\frac{(\theta-\theta_w)}{(\theta_*-\theta_w)}, & \text{if } \theta_g < \theta \le \theta_w \\ A_{\max} & \text{if } \theta \ge \theta_*. \end{cases} \tag{8}$$

The actual transpiration (Tr) is determined from the carbon assimilation and the appropriate WUE term:

$$\mathrm{Tr} = \frac{A}{\mathrm{WUE}}(18.016). \tag{9}$$

The total biomass of the woody species is calculated as the previous biomass plus the sum of the daily assimilation in any year. Whereas the grass biomass is reinitialized each year. Extreme water stress can force senescence of the vegetation through exceeding a threshold based on the number of days of stress (15 days for grass and 75 days for woody species). At the end of each year, the cumulative biomass is added to the woody species and is translated to a fractional coverage (Fv_t) based on a carrying load concept of a maximum amount of woody biomass that is allowed in the model.

The occurrence of fire is modeled as a uniform random variable on an annual basis with frequency λ_f (D'Odorico et al., 2006). The occurrence of the fire is then uniformly distributed over days of the years 80 (21 March) to 130 (10 May), representative of spring burning that is common in the central United States (Blair et al., 2014). This is a simplification of the observed burning on the KON watershed that over the 1983–2016 period had a mean day of year (DOY) of 108 ± 14 days and ranged from DOY 56 to DOY 133. The vast majority of prescribed fires that are performed during these conditions result in low-intensity fire, with the goal of removing litter but reducing potential risks. Similarly, most wildfires still occur in the early spring, when high-intensity fires are less likely (Krueger et al., 2016). Therefore, to make our model more applicable to the current fire regime, we only consider explicit variation in fire frequency rather than intensity. It should be noted, however, that high-intensity fires could be a more effective means of controlling woody vegetation.

A positive feedback is incorporated between the fire intensity (ω_f) and grass fraction to account for the reduction in fuel load as the grass fraction decreases:

$$\omega_f = Fv_g \frac{X}{\omega_0(1-\exp(-2/\omega_0))}, \tag{10}$$

where Fv_g is the grass fraction and X is an exponentially distributed random variable with likelihood ω_0 (D'Odorico et al., 2006).

If a fire occurs, all of the grass biomass is consumed, while the woody biomass is diminished in relation to the fire intensity as

$$\frac{B_t}{dt} = (1-\omega_f)B_t. \tag{11}$$

In order to examine the relative controls of precipitation frequency (λ), intensity (α), and fire frequency (λ_f) on woody encroachment in grassland environments, we iterated the model over five values of each of these parameters (Table 1) resulting in a combination of 125 simulations. Each simulation was conducted for a period of 100 years with a daily time step. All simulations are initialized with 100% grass cover, and as woody encroachment occurs, the grass fraction is assumed to occupy any space that is not tree covered. While these parameters are stochastic, there is no long-term trend in the model simulations and these simulations do not represent climate change scenarios, but rather a long-term simulation to examine the stable woody fraction that may result under that particular combination of precipitation and fire.

The model simulations are conducted over a parameter space that encompasses a wide range of annual precipitation and fire frequencies ranging from 180 to 2500 mm/yr for total annual precipitation and fire frequencies ranging from every year to one fire every 16 years. While the 2500 mm/yr value is obviously extreme

Table 1
Parameter Values for Precipitation Magnitude (α), Frequency (λ), and Fire Frequency (λ_f) Used in the Simulations

Precipitation intensity (α) (mm/event)	Precipitation frequency (λ) (events/day)	Fire frequency (λ_f) (events/year)/(return interval in years)
6	0.05	0.0625/16
7	0.1	0.125/8
8	0.2	0.25/4
9	0.35	0.5/2
10	0.5	1.0/1

for the existence of a grassland, we chose to extend the parameter values beyond the expected range in order to examine model behavior at these values. Each simulation was initialized in a grassland state with a small randomly generated tree fraction (10% probability of new establishment woody species) and allowed to vary over time in relation to the stochastic rainfall and fire forcing events. Each year, there is a likelihood of tree life establishing itself within the simulation (10%) and a small possibility of tree mortality (0.5%).

2.3. Diagnosing Stability With Lyapunov Exponents

While the model was validated using data from the central United States grasslands, one objective of this work is to examine the role of precipitation and fire variability on the fractions of grass and tree that result in the model. To this end, we utilized Lyapunov exponents to examine the 125 model simulations spanning 100 years for each of the fire and precipitation parameter values. This method allows us to examine the average exponential rate of growth (positive Lyapunov exponent) or decay (negative Lyapunov exponent) in an embedded time series to quantify the stability with respect to the initial (grassland) state in the simulations. We conducted the Lyapunov exponent analysis in two ways. First, we computed local, normalized Lyapunov exponents across a range of timescales (the divergence timescale) to assess the sensitivity of selected daily model variables to the stochastic forcing. Second, we examined the global Lyapunov exponent of the woody fraction, determined on an annual basis, to quantify the overall stability of the woody cover in relation to the α, λ, and λ_f parameters. This results in a quantitative measure of the stability of the grassland system under that particular parameter combination.

Our approach here is to create different scenarios based on precipitation frequency and intensity, and fire frequency and employ the largest Lyapunov exponent to determine the relative sensitivity of these different scenarios to stochastic perturbations. Since the largest Lyapunov exponent is an average over the whole time interval of interest (100 years), we also consider averages over shorter time intervals to uncover seasonal dependencies on the sensitivities. Here we focus on the largest Lyapunov exponent as opposed to several of the largest Lyapunov exponents. This is motivated by the importance of the largest growth rate and the fact that obtaining more Lyapunov exponents from time series data remains somewhat problematic with embedding techniques due to the need to separate the actual Lyapunov exponents obtained from the spurious ones.

We utilized approximations of the largest Lyapunov exponent to examine the stability of woody vegetation fraction from the time series of model output. For a time series of variable $x_{t+1} = f(x_t)$, the largest Lyapunov exponent can be approximated on a timescale of length N as

$$\lambda_1 = \frac{1}{N}\sum_{j=0}^{N-1} \log(|f'(x_j)|). \tag{12}$$

To approximate the largest Lyapunov exponent from the model time series, the approach of Rosenstein et al. (1993) was used for an embedded time series $\{X_t\}$:

$$X_t = (x_t, x_{t-J}, \ldots, x_{t-(M-1)*J}), \tag{13}$$

where J is the time delay and M is the embedding dimension.

The approach taken here is similar to that utilized in Graham et al. (2007) and requires determining appropriate values of the time delay and the embedding dimension. The embedding dimension M was calculated using

a method based upon false nearest neighbors (Kennel et al., 1992). This approach examines whether points that are near neighbors in one dimension are also near neighbors in the next higher embedding dimension. If not, then the image had not been fully unfolded. If all near neighbors remain so, then the unfolding is complete and the dimension is established. We found the results to be robust in various time delays and embedding dimensions. The results reported here were obtained with $J = 2$ and $M = 15$.

To approximate the largest Lyapunov exponent, the idea is to measure the distance ($\delta = \|X_j - X_k\|$) between the neighboring points from times in the embedded space (j and k) as

$$\|X_{i+t} - X_{j+t}\| = \delta e^{\lambda_1 t}, \tag{14}$$

where λ_1 is the approximation of the largest Lyapunov exponent.

At each time (j) the nearest neighbor in embedding space (that is not too close in time) is selected ($d_j(0) = \min_{X_k} \|X_j - X_k\|$). As time is stepped forward, the distance between those neighboring points is calculated as

$$d_j(i) = \|X_{j+i} - X_{k+i}\| \equiv d_j(0)e^{\lambda_1 \cdot i}. \tag{15}$$

The logarithm of the average distance (in time) with fixed divergence time (i) is calculated as $y(i) = <\log(d_j(i))>$. Then the global largest Lyapunov exponent is approximated by the slope of the linear least squares fit to $\{i, y(i)\}$. For the global largest Lyapunov exponent, we fit based upon divergence times from 1 day to 5 years using increments of 30 days. We also approximate average convergence/divergence over different divergence times to determine seasonal cycles of convergence/divergence. In both cases we are measuring the sensitivity with respect to perturbations in a given state value either globally over a long-time interval or locally over a fixed time interval.

We calculate both approximations of local and global largest Lyapunov exponent. The local largest Lyapunov exponent for divergence time i is approximated by the slope of $\tilde{y}(i)$ where

$$\tilde{y}(i) = <\log(d_j(i)/d_j(0))> \approx \tilde{\lambda}_1(i) \cdot i \tag{16}$$

and thus given approximately by $\tilde{\lambda}(i)$. The slope of these curves provides a type of local largest Lyapunov exponent that measures the average rate of growth (positive slope) or decay (negative slope) over the given divergence time. This is similar to a stability spectrum based upon the so-called Steklov (or windowed) averages (see Dieci & Van Vleck, 2006, 2015).

3. Results and Discussion

3.1. Comparison With Eddy Covariance and Historical Woody Fraction Observations

We compared the model to eddy covariance observations by forcing the model with observed precipitation from the Konza Prairie sites to verify the daily fluxes computed in the model. The model was run for the period of 1 January 2008 through 31 December 2014. Given that the governing hypothesis of the model is that the carbon and water cycling is controlled primarily by water limitation (i.e., no nutrient limitation), it is not expected that the model and observations will match perfectly.

Time series of the evapotranspiration (ET) and gross primary production (GPP) fluxes are shown in Figure 2 for both the annually burned and the 4 year burn eddy covariance sites. In general, the model captured the seasonal cycle and dynamic range of the fluxes. The evaporative flux was underestimated in times of high evaporative demand (summer). The overall model performance is acceptable with correlations of 0.41 and 0.47 for the evaporative fluxes at the annually burned and 4 year burn sites, respectively. The correlation for the GPP fluxes was higher at both sites, 0.60 at the annual site, and 0.63 for the 4 year burn site, although peak levels were also slightly underestimated with respect to the tower observations.

The record length of eddy covariance observations is too short of a record to examine the interannual trend in woody cover. Therefore, we conducted a 50 ensemble member series of model simulations using observed precipitation and fire occurrence data for three watersheds at the Konza Prairie (Figure 3) with historical observations of woody cover (Briggs et al., 2005). Since observations of fire intensity are not available, these were stochastically determined within the model. The three watersheds consisted of an annually burned (KON), 4 year burn (KFB), and 20 year burn site (20B). The goal of this comparison was to assess model variability, rather than to perfectly replicate the observed woody fraction data. Figure 3 illustrates the 25–50% and 0.05–0.95% confidence intervals around the modeled woody fraction through time. In general, the model

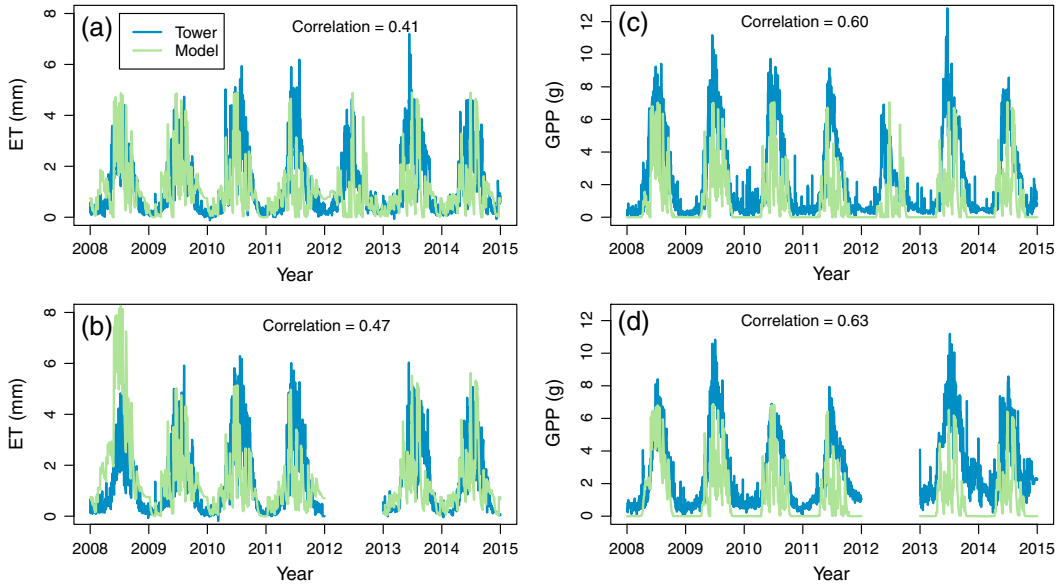

Figure 2. Comparison of model output with eddy covariance data for (a) annually burned site US-KON ET in millimeter, (b) annually burned US-KON GPP (g CO_2), (c) 4 year burn site US-KFB ET (mm), and (d) 4 year burn site US-KFB GPP (g CO_2).

performed well, correctly estimating the very low woody fraction on the annually burned site. The 4 year model simulations fall within the 0.25–0.75% confidence interval, while the 20 year burn simulation is overestimated. Within the 20 year and 4 year simulations, the model shows an increase in the woody fraction from the beginning of the simulations, while the observations show a lag in the onset of encroachment. This is most pronounced within the 20B watershed, where woody encroachment does not begin (fraction of woody species >10%) until 2000. However, once the encroachment begins, the rate of increase in the watershed is 0.034 (%/year) that is comparable to the rate of increase in the model (0.030%/year). Given that the overall purpose of the model is to investigate the long-term stability of the model (e.g., after 100 years) rather than the timing of the onset of encroachment, this is determined to be adequate. Over longer timescales, other studies (Briggs et al., 2002) have shown that long fire intervals converge to closed forests.

These model validations illustrate that the model may underestimate the fluxes; however, the general dynamics of woody encroachment are well characterized. These results are consistent with other findings in the central U.S. that find that a fire frequency of 1–2 years corresponds to very little woody encroachment and above 3.5–4 years resulting in encroachment (Bowles and Jones, 2013; Ratajczak, Nippert, Briggs et al., 2014). This gives confidence in interpreting the model output in terms of the responses to variation in the environmental forcings.

3.2. Assessing the Roles of Fire and Precipitation

Given that the model generally captures the dynamics at each site, we are confident in using the model to assess the carbon and water cycle impacts of alterations to the precipitation timing, magnitude, and fire frequency.

As a first assessment, the temporal evolution of the woody fraction is presented in Figure 4 for three different precipitation regimes, including a low annual precipitation regime ($\alpha = 1$, $\lambda = 0.05$, MAP = 178.6 mm), an intermediate level of annual precipitation, characteristic of the Konza Prairie site ($\alpha = 0.8$, $\lambda = 0.2$, MAP = 827.1 mm), and a high mean annual precipitation environment ($\alpha = 0.6$, $\lambda = 0.5$, MAP = 2423.9 mm). Note that the values of mean annual precipitation given here are actual values from a specific realization of the model and not the expected value, given the precipitation parameters. In addition, each of the five fire frequency values ranging from every year to every 16 year occurrence probabilities is illustrated for each precipitation combination. Woody expansion is generally suppressed in the low precipitation simulations (Figure 4a), reaching approximately 50% in the less frequent burn regimes. In the intermediate annual precipitation simulations (Figure 4b), woody encroachment becomes higher, reaching 100% cover in the 16 year burn. As expected a high woody fraction is more consistently seen in the higher precipitation regime

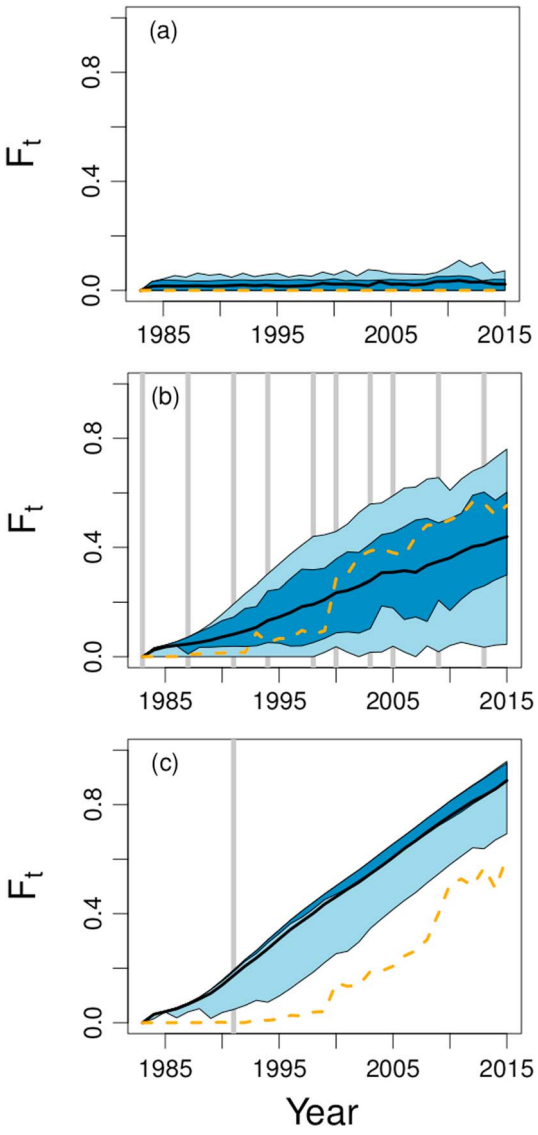

Figure 3. Woody tree fraction modeled and observed at Konza LTER for watersheds that have (a) annual (watershed 1D), (b) 4 year (watershed 4B), and (c) 20 year (watershed 20B) burn frequencies. Black line indicates the mean of a 50-member ensemble of model simulations forced with observed precipitation and burn occurrence. Lighter shading region indicates 0.05 and 0.95 probability range, while darker region indicates 0.25 and 0.75 range of woody fraction in model simulations. Gray lines indicate burn years in the 4 year and 20 year watersheds. Orange dashed line indicates observed values of woody fraction.

(Figure 4c) and with a burn frequency of 8 or more years. Woody fraction exhibits greater variability with annual and biennial burn regimes.

Next, we examined the full variability in woody encroachment across the full parameter space of precipitation frequency and intensity and fire frequency. One hundred years of daily precipitation was generated for each α and λ combination (Figure 5). The maximum woody fraction over the 100 year simulation for each combination of α, λ, and λ_f is shown in Figure 6. The control exerted on woody fraction by the fire regime is obvious, with lower values of λ_f (Figure 6, first and second panels) almost always resulting in 100% woody cover during the simulation and an annual burn regime (third to fifth panels) resulting in very low fractions of woody cover. For the 4 year burn regime, the model resulted in the full range of woody fraction, with the woody fraction varying with mean annual precipitation. Lower precipitation amounts corresponded to lower woody fraction; and increasing precipitation corresponded to increases in woody fraction (Eldridge et al., 2011). Higher-frequency burn regimes (1 and 2 year frequencies) corresponded to drastically less woody cover. Note that only in the intermediate burn regimes of 2 years and in particular 4 years is a relationship between woody cover and the precipitation timing and magnitude observed, with woody fraction increasing from the upper left corner of the panel (lower annual precipitation values) to the lower right corner (higher annual precipitation). It is important to note that these values are the results of a single, 100 year simulation for each parameter combination; given the stochastic forcing in the model, different realizations are likely to result in some variation in the maximum woody fraction. Therefore, these results should be considered as being indicative of the general trend across the parameter space rather than absolute values.

3.3. Stability Analysis Using Lyapunov Exponents

The goal of this work was to assess the overall stability of the carbon flux, water flux, and grass and woody fractions in response to stochastic variability in the precipitation and burning regimes. To this end, we utilized the Lyapunov exponents. First, we examined the variation in the local Lyapunov exponents related to selected model state variables related to water and carbon cycling. These variables were soil moisture (θ), woody transpiration (Tr_t), bare soil evaporation (Es), and grass carbon assimilation (A) within each realization of the model.

In Figure 7 we plot the divergence time i versus the logarithm of the time-averaged logarithm of the divergence distance. Here the $\bar{y}(i)$ as defined in equation (16) has been normalized by the initial lag ($J = 0$) in order to examine relative variability across different precipitation and fire regimes as a function of the divergence timescale. Figure 7 illustrates the behavior of the normalized local Lyapunov exponents for a subset of the precipitation magnitudes, frequencies, and burn frequencies as a function of the divergence timescale. Recall that the local Lyapunov exponent is the local slope in Figure 7 and not the absolute values displayed in the figure. The model exhibited a strong periodicity in the variation of the Lyapunov exponents as a function of divergence timescale. In general, the Lyapunov exponents became smaller (decreased local rates of change, e.g., periodicity) with increasing precipitation (moving from Figure 7, left column, to Figure 7, right column).

Over short time lags, the variation in the normalized Lyapunov exponent (slope in Figure 7) indicates a relative increase or decrease in the stability. A positive slope indicates more unstable over those timescales (i), while a decreasing slope indicates the variable is becoming less unstable with respect to fluctuations from the initial conditions. Positive values indicate unstable regimes and an increase in the distance between initial neighbors in the parameter space with increasing time. For low annual precipitation (Figures 7a, 7d, and 7g)

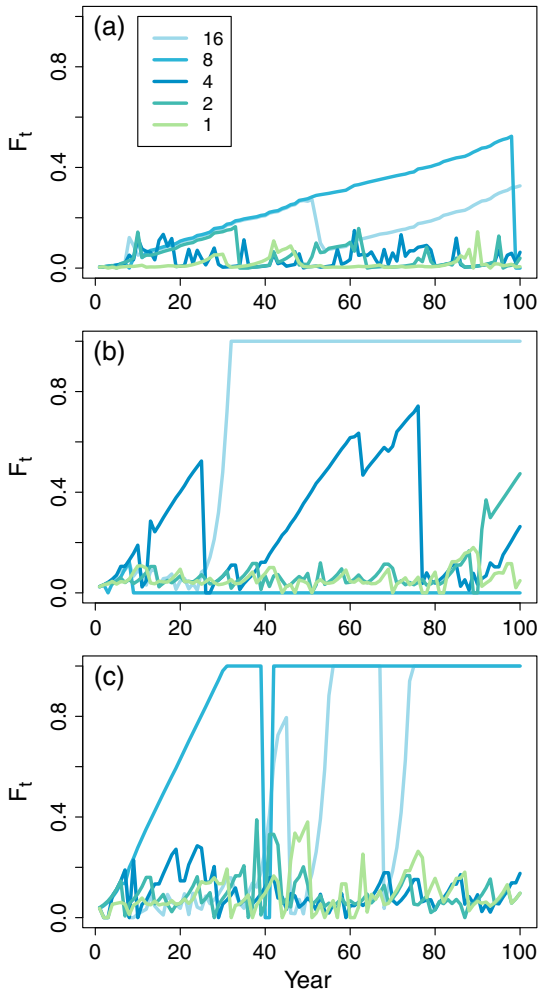

Figure 4. Woody tree fraction for different burn frequencies (1, 2, 4, 8, and 16 years) for different combinations of precipitation timing and magnitude. (a) Low annual precipitation (α = 1, λ = 0.05, MAP = 178.6 mm). (b) Intermediate annual precipitation (α = 0.8, λ = 0.2, MAP = 827.2 mm). (c) High annual precipitation (α = 0.6, λ = 0.5, MAP = 2423.9 mm).

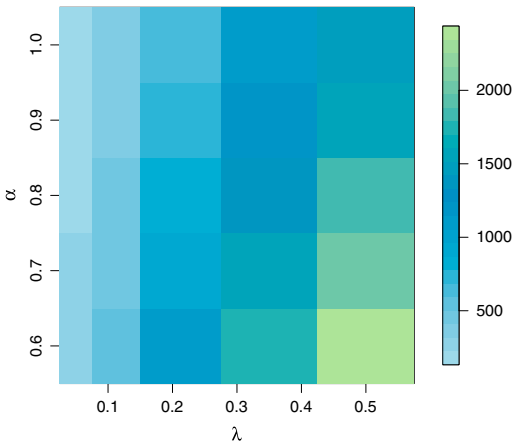

Figure 5. Mean annual precipitation (millimeter) as a function of precipitation intensity (α) and precipitation frequency (λ) used in the simulations.

there was a prevalent oscillation frequency of approximately 6 months in all variables, most notably in the woody transpiration and the bare soil evaporation. As precipitation increased to intermediate amounts (Figures 7b, 7e, and 7h) this periodicity was diminished, particularly for the soil moisture and grass assimilation, thus indicating that the slopes are generally decreasing and indicating more stable conditions. This was continued at the highest precipitation values considered (Figures 7c, 7f, and 7i) where the periodicity was lost.

Increasing burn frequency is illustrated by progressing from Figure 7 (top row) to Figure 7 (bottom row). As burn frequency increased, there was little influence over the stability of the dependent variables in the model (e.g., compare Figures 7a, 7d, and 7g). Figures 7e–7i demonstrate strong discontinuities in the grass assimilation. These occurred at multiples of the imposed phenological cycle and are likely the result of the combined effects of the phenology and precipitation regime. These results indicate that as water availability increases, seasonal variability becomes less pronounced in the model output. This is in line with a governing assumption of the model: that water is a limiting resource. In conjunction with the reduction in the seasonal periodicity, the Lyapunov exponents generally decrease and the system is generally becoming more stable.

What is observed in Figure 7 is that for some parameter configurations these local type Lyapunov exponents produce an annual pattern with seasonal variations. In Figure 7 some variables, for example, grass assimilation, woody transpiration, and top layer soil moisture, have two peaks per year while other variables, for example, bare soil evaporation, have a single peak per year. Two peaks in these plots correspond to instability (sensitivity with respect to perturbations in that variable) over divergence times of 0–3 months, 6–9 months, 12–15 months, etc., while one peak per year corresponds to instability over divergence time of 0–6 months, 12–18 months, etc. We emphasize that it is the slope in Figure 7 that corresponds to local type Lyapunov exponent (exponential rate of convergence/divergence) so that a positive slope corresponds to a positive local Lyapunov exponent and exponential divergence on this timescale and similarly for a regions where the slope is negative. We also note that all computations reported here were performed using a single realization of the rainfall and fire (stochastic) forcing. Qualitatively similar results were obtained when forcing using other instances from the same parameterization of the stochastic forcing.

The stability of the woody fraction was investigated using global Lyapunov exponents (Figure 8). Burn frequency and precipitation frequency strongly controlled the stability of the woody tree fraction. As precipitation frequency increased, the Lyapunov exponent of the woody fraction decreased (Figure 8a). This indicates that woody encroachment was becoming more stable. In contrast, as the burn frequency became higher, woody species were less favored and became more unstable (Figure 8b). There appears to be no relationship between the stability of woody cover and precipitation magnitude (not shown), in contrast to the recent findings of Good and Caylor (2011) and Xu et al. (2015). It should be noted that February et al. (2013) found that additional precipitation increased the competitiveness of grasses over trees, similar to our findings.

Figure 9 illustrates the mean Lyapunov exponent across all of the variability in precipitation timing, magnitude, and burn frequency. Within a given burn regime (panels in Figure 9) there appeared little significant variability

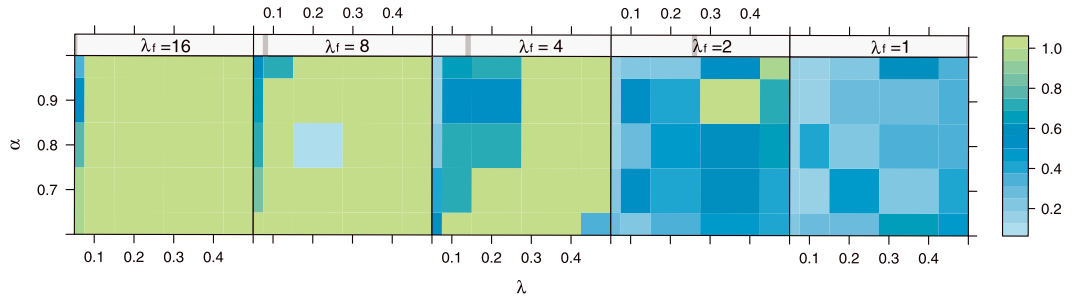

Figure 6. Variation in maximum tree fraction (%) as a function of precipitation intensity (α), precipitation frequency (λ), and fire frequency (λ_f).

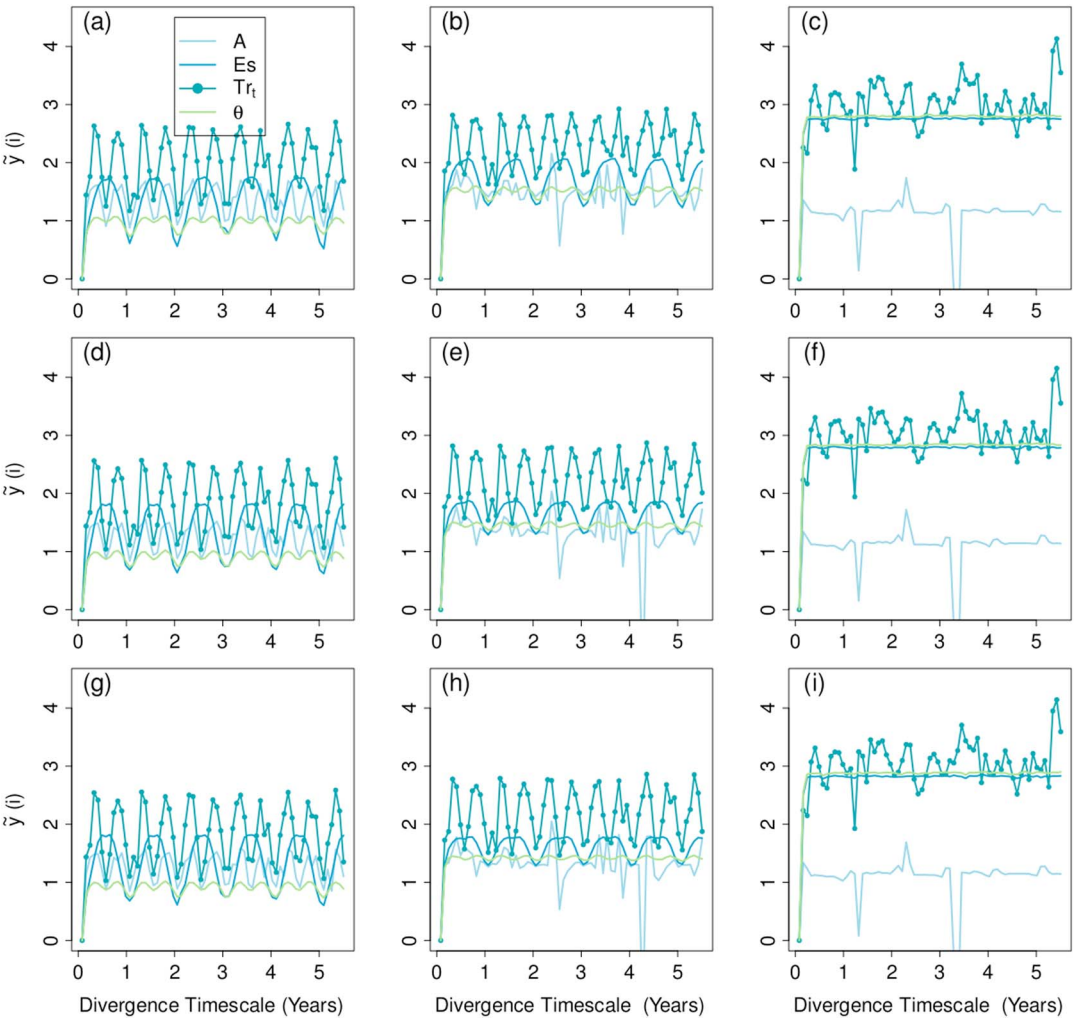

Figure 7. Largest local Lyapunov exponent as a function of divergence timescale (i) approximated by the slope of the curve $\tilde{y}(i)$. Model variables A grass assimilation, E_s bare soil evaporation, Tr_t woody transpiration, and θ top layer soil moisture. Columns correspond to selected precipitation magnitude and frequency values as in Figure 3. (a, d, and g) The low mean annual precipitation ($\alpha = 1$, $\lambda = 0.05$, MAP = 178.6 mm), (b, e, and h) The intermediate mean annual precipitation ($\alpha = 0.8$, $\lambda = 0.2$, MAP = 827.2 mm), and (c, f, and i) The high annual precipitation ($\alpha = 0.6$, $\lambda = 0.5$, MAP = 2423.9 mm). Rows correspond to selected fire frequency values: (a–c) The 16 year return frequency, (d–f) the 4 year burn interval, and (g–i) the 1 year burn frequency.

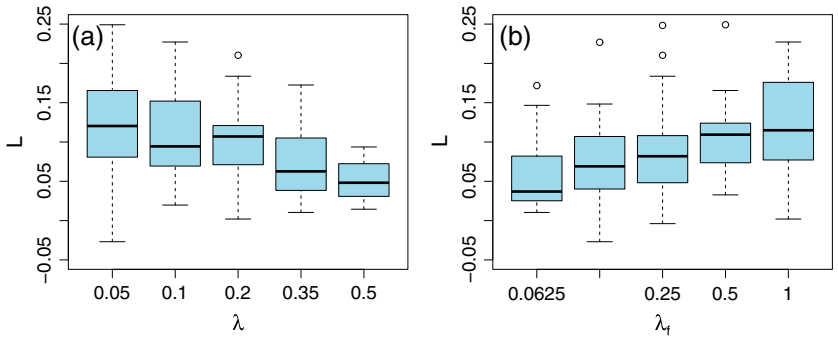

Figure 8. The distribution of the global Lyapunov exponent (L) for woody tree fraction (Fv_t) as a function of (a) precipitation frequency (λ) and (b) fire frequency (λ_f).

due to the precipitation regime. The Lyapunov exponents of the woody cover indicate an increase with decreasing precipitation frequency and increasing fire frequency. Since the model is initialized in a grass state (low woody cover), these positive Lyapunov exponents indicate an instability with respect to the model simulations, the most instability corresponding to the highest woody cover in the end state of the model. Thus, we conclude, that while precipitation frequency is important, in this particular case the fire frequency appears to exert a more systematic influence over the long-term stability of the grass-woody system as exemplified in the central United States.

It is important to note that this modeling framework does not consider the impact of grazing on the expansion of woody species. While grazing is an important determinate of woody coverage globally, grazing does not appear to be a primary factor within the central Great Plains of the United States that is the focus of this study (Briggs et al., 2005). In an observational study based at the Konza Prairie, Ratajczak, Nippert, Briggs et al. (2014) found that while grazing may facilitate some minor shrub establishment in high-frequency fire regimes, there is an adverse effect in lower frequency (4 and 20 year burn regimes) and that overgrazing was not a contributor to woody encroachment at KPBS, as the rate and magnitude of encroachment are similar among grazed and ungrazed locations. These results are supported by a modeling study from Fuhlendorf et al. (2008) who found that fire frequencies less than 15 years were sufficient in maintaining the grassland state of the more southern productive grassland/savanna regardless of grazing intensity. Therefore, the lack of consideration giving to grazing is justified in the first-order modeling framework considered here. Indeed, the addition of fire already represents a major addition to analogous models, which tend to focus primarily on ecohydrology (Xu et al., 2015; Ying et al., 2017). However, in future model development, the addition of a grazing parameterization will likely increase the applicability of the model to assess the impacts of woody expansion globally.

The model simulations do not explicitly differentiate between different species of woody expansion. Differences among species and woody growth forms (shrubs versus trees and resprouters versus nonresprouters) are likely to impact the dynamics of expansion by woody plants into grasslands. As a consequence, the fire frequency required to maintain a particular ecosystem state (grassland, shrubland, and woodland) varies according to species and growth forms compared (Ratajczak, Nippert, Briggs et al., 2014). Future model improvements could more explicitly account for the different strategies utilized by shrubs and deciduous trees

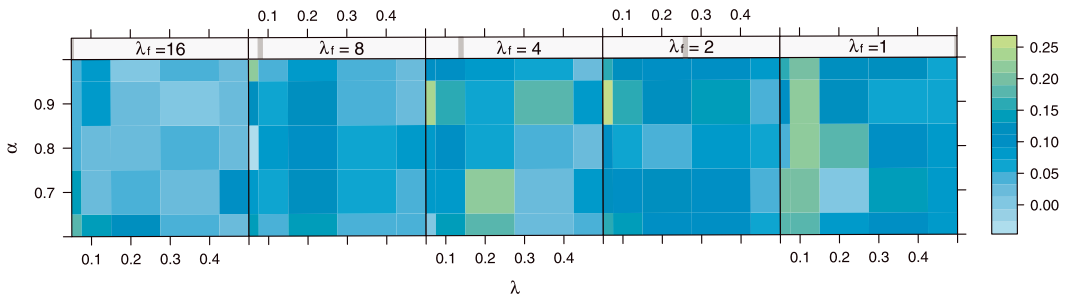

Figure 9. The distribution of the global Lyapunov exponent (L) for woody tree fraction (Fv_t) as a function of precipitation magnitude (α), frequency (λ), and fire frequency (λ_f).

by altering carrying capacity, water use efficiency, and the likelihood of propagation. A more explicit treatment of the woody species may also improve the model's capability to correctly simulate the lag in the onset of the woody expansion observed in the 20 year burn watershed.

In addition, the model framework presented here does not consider the role of climate change on the stability of the woody cover. Factors such as CO_2 fertilization and changes in the local temperature and precipitation are important in determining how climate change and human management of grassland systems (Sankaran et al., 2005; Twidwell, Rogers et al., 2013) will impact systems experiencing woody encroachment and should be incorporated into future model development. Thus, the simulations and results presented here are the end-member states of the woody fraction in response to a stochastically constant fire and precipitation variability. While this has implications for how these systems might respond under climate change, the lack of CO_2 enrichment effects and other biogeochemistry feedbacks in the model limits that interpretation. However, as woody encroachment is increasing in grasslands and savannas around the globe, these results point to the potential of using fire as a control mechanism that is consistent with previous research (Twidwell, Fuhlendorf et al., 2013). Climate change may alter the relative benefits of woody species to access deeper water reservoirs due to changes in the local precipitation environment (means as well as the seasonal distribution), an increase in extreme events such as drought and flooding, and increasing atmospheric CO_2 that can all alter the distribution of water with depth in the soil (Schlaepfer et al., 2017). The alteration of soil water will have profound impacts on the potential expansion of woody species (Honda & Durigan, 2016). These factors that undoubtedly interact in complex and nonlinear ways should be the focus of additional research.

4. Conclusions

A new model is proposed to examine the stability of woody encroachment in response to stochastic precipitation and fire occurrence in grasslands in the central United States. When the potential for woody plant expansion is accounted for, we found that the rainfall frequency was more important than the magnitude of the individual rainfall events. However, when we considered the additional role of fire disturbance, these results indicate that fire frequency exerts a dominant control on the existence of woody cover across a wide range of mean annual precipitation values, leading to fire being a dominant control of water and carbon fluxes as well (Barger et al., 2011; Knapp et al., 2008). For instance, remotely sensed estimates of fire frequency in the vicinity of our calibration site estimate that 45% of the 2,775,095 ha of grasslands are burned at a fire interval >4 years and 32% are burned at an interval >10 years (Ratajczak et al., 2016). Therefore, if our model results hold, then almost half of these grasslands are susceptible to woody encroachment, even if precipitation declines. These trends in fire frequency are mirrored at larger scales (Nowacki & Abrams, 2008). These results indicate that stable alternate states are present in the woody-grass fraction continuum, and that intermediate states in woody cover can be maintained through specific precipitation and fire regimes.

It remains to be seen to what extent increases in fire frequency can be used to reverse areas that have already been encroached (Ratajczak et al., 2016). While there are many sociological complications with human's relationship with burning, Twidwell, Rogers et al., (2013) demonstrate the benefits of the rise of burn cooperatives across the central plains. We have shown that high-frequency burning may be an effective strategy for limiting the expansion of woody species within the U.S. Great Plains.

Acknowledgments
This work was funded through support from the LTER program at the Konza Prairie Biological Station (DEB-0823341). In addition, the US-KON and US-KFB Ameriflux sites are operated as a portion of the Konza Core Ameriflux site by N. A. B. sponsored by the U.S. Department of Energy under a subcontract from DE-AC02-05CH11231. The work of E. S. V. V. was supported in part by NSF grant DMS-1419047. Z. R. was supported by NSFDBI-1402033. All data used in this analysis are available through the Konza Prairie LTER data site (http://www.konza.ksu.edu/knz/pages/data/knzdata.aspx) or the Ameriflux site (http://ameriflux.lbl.gov/).

References

Archer, S., Schimel, D. S., & Holland, E. A. (1995). Mechanisms of shrubland expansion: Land use, climate or CO_2? *Climatic Change*, *29*(1), 91–99.

Barger, N. N., Archer, S. R., Campbell, J. L., Huang, C.-Y., Morton, J. A., & Knapp, A. K. (2011). Woody plant proliferation in North American drylands: A synthesis of impacts on ecosystem carbon balance. *Journal of Geophysical Research*, *116*, G00K07. https://doi.org/10.1029/2010JG001506

Blair, J., Nippert, J., & Briggs, J. (2014). Grassland ecology. In R. K. Monson (Ed.), *Ecology and the environment, The plant sciences* (Vol. 8, pp. 389–423). New York, NY: Springer Science+Business Media.

Bond, W. J. (2008). What limits trees in C4 grasslands and savannas? *Annual Review of Ecology, Evolution, and Systematics*, *39*(1), 641–659.

Bowles, M. L., & Jones, M. D. (2013). Repeated burning of eastern tallgrass prairie increases richness and diversity, stabilizing late successional vegetation. *Ecological Applications*, *23*(2), 464–478.

Briggs, J. M., Hoch, G. A., & Johnson, L. C. (2002). Assessing the rate, mechanisms, and consequences of the conversion of tallgrass prairie to Juniperus virginiana forest. *Ecosystems*, *5*(6), 578–586.

Briggs, J. M., Knapp, A. K., Blair, J. M., Heisler, J. L., Hoch, G. A., Lett, M. S., & McCarron, J. K. (2005). An ecosystem in transition. Causes and consequences of the conversion of mesic grassland to shrubland. *BioScience*, *55*(3), 243–254.

Brovkin, V., Claussen, M., Petoukhov, V., & Ganopolski, A. (1998). On the stability of the atmosphere-vegetation system in the Sahara/Sahel region. *Journal of Geophysical Research*, *103*(D24), 31,613–31,624.

Brunsell, N. A., Nippert, J. B., & Buck, T. L. (2014). Impacts of seasonality and surface heterogeneity on water-use efficiency in mesic grasslands. *Ecohydrology*, *7*, 1223–1233.
Claussen, M., Kubatzki, C., Brovkin, V., Ganopolski, A., Hoelzmann, P., & Pachur, H. J. (1999). Simulation of an abrupt change in Saharan vegetation in the mid-Holocene. *Geophysical Research Letters*, *26*(14), 2037–2040.
Cushing, J. M., Costantino, R. F., Dennis, B., Desharnais, R., & Henson, S. M. (2002). *Chaos in ecology: Experimental nonlinear dynamics*. Theoretical Ecology Series: Elsevier Science.
Dakos, V., Benincà, E., van Nes, E. H., Philippart, C. J. M., Scheffer, M., & Huisman, J. (2009). Interannual variability in species composition explained as seasonally entrained chaos. *Proceedings of the Royal Society of London B: Biological Sciences*, *276*(1669), 584–2880.
Dekker, S. C., Rietkerk, M., & Bierkens, M. F. P. (2007). Coupling microscale vegetation–soil water and macroscale vegetation–precipitation feedbacks in semiarid ecosystems. *Global Change Biology*, *13*(3), 671–678.
Dieci, L., & Van Vleck, E. S. (2006). Lyapunov and Sacker–Sell spectral intervals. *Journal of Dynamics and Differential Equations*, *19*(2), 265–293.
Dieci, L., & Van Vleck, E. S. (2015). Lyapunov exponents: Computation. In *Encyclopedia of applied and computational mathematics* (pp. 834–838). Berlin Heidelberg: Springer-Verlag. https://doi.org/10.1007/978-3-540-70529-1
D'Odorico, P., Laio, F., & Ridolfi, L. (2006). A probabilistic analysis of fire-induced tree-grass coexistence in savannas. *American Naturalist*, *167*(3), E79–E87.
D'Odorico, P., Okin, G. S., & Bestelmeyer, B. T. (2012). A synthetic review of feedbacks and drivers of shrub encroachment in arid grasslands. *Ecohydrology*, *5*(5), 520–530.
Eldridge, D. J., & Soliveres, S. (2014). Are shrubs really a sign of declining ecosystem function? Disentangling the myths and truths of woody encroachment in Australia. *Australian Journal of Botany*, *62*(7), 594–15.
Eldridge, D. J., Bowker, M. A., Maestre, F. T., Roger, E., Reynolds, J. F., & Whitford, W. G. (2011). Impacts of shrub encroachment on ecosystem structure and functioning: Towards a global synthesis. *Ecology Letters*, *14*(7), 709–722.
February, E. C., Higgins, S. I., Bond, W. J., & Swemmer, L. (2013). Influence of competition and rainfall manipulation on the growth responses of savanna trees and grasses. *Ecology*, *94*(5), 1155–1164.
Fuhlendorf, S. D., & Engle, D. M. (2004). Application of the fire–grazing interaction to restore a shifting mosaic on tallgrass prairie. *Journal of Applied Ecology*, *41*(4), 604–614.
Fuhlendorf, S. D., Archer, S. A., Smeins, F., Engle, D. M., & Taylor, C. A. (2008). The combined influence of grazing, fire, and herbaceous productivity on tree–grass interactions. In *Western North American Juniperus Communities* (pp. 219–238). New York, NY: Springer.
Good, S. P., & Caylor, K. K. (2011). Climatological determinants of woody cover in Africa. *Proceedings of the National Academy of Sciences of the United States of America*, *108*(12), 4902–4907.
Graham, D. W., Knapp, C. W., Van Vleck, E. S., Bloor, K., Lane, T. B., & Graham, C. E. (2007). Experimental demonstration of chaotic instability in biological nitrification. *The ISME Journal*, *1*(5), 385–393.
Higgins, S. I., Scheiter, S., & Sankaran, M. (2010). The stability of African savannas: Insights from the indirect estimation of the parameters of a dynamic model. *Ecology*, *91*(6), 1682–1692.
Holdo, R. M., & Nippert, J. B. (2015). Transpiration dynamics support resource partitioning in African savanna trees and grasses. *Ecology*, *96*(6), 1466–1472.
Honda, E. A., & Durigan, G. (2016). Woody encroachment and its consequences on hydrological processes in the savannah. *Philosophical Transactions of the Royal Society of London. Series B: Biological Sciences*, *371*(1703), 20150313. https://doi.org/10.1098/rstb.2015.0313
Kennel, M. B., Brown, R., & Abarbanel, H. D. (1992). Determining embedding dimension for phase-space reconstruction using a geometrical construction. *Physical Review A*, *45*(6), 3403–3411.
Knapp, A. K., & Smith, M. D. (2001). Variation among biomes in temporal dynamics of aboveground primary production. *Science*, *291*(5503), 481–484.
Knapp, A. K., Briggs, J. M., Collins, S. L., Archer, S. R., Bret-Harte, M. S., Ewers, B. E., … Cleary, M. B. (2008). Shrub encroachment in North American grasslands: Shifts in growth form dominance rapidly alters control of ecosystem carbon inputs. *Global Change Biology*, *14*(3), 615–623.
Koerner, S. E., & Collins, S. L. (2014). Interactive effects of grazing, drought, and fire on grassland plant communities in North America and South Africa. *Ecology*, *95*(1), 98–109.
Krueger, E. S., Ochsner, T. E., Carlson, J. D., Engle, D. M., Twidwell, D., & Fuhlendorf, S. D. (2016). Concurrent and antecedent soil moisture relate positively or negatively to probability of large wildfires depending on season. *International Journal of Wildland Fire*, *25*(6), 657–12.
Kulmatiski, A., & Beard, K. H. (2013). Woody plant encroachment facilitated by increased precipitation intensity. *Nature Climate Change*, *3*(9), 833–837.
Lehmann, C. E. R., Anderson, T. M., Sankaran, M., Higgins, S. I., Archibald, S., Hoffmann, W. A., … Bond, W. J. (2014). Savanna vegetation-fire-climate relationships differ among continents. *Science*, *343*(6170), 548–552.
Logan, K. E., & Brunsell, N. A. (2015). Influence of drought on growing season carbon and water cycling with changing land cover. *Agricultural and Forest Meteorology*, *213*, 217–225.
Molz, F., & Faybishenko, B. (2013). Increasing evidence for chaotic dynamics in the soil-plant-atmosphere system: A motivation for future research. *Procedia Environmental Sciences*, *19*, 681–690.
Myers-Smith, I. H., Forbes, B. C., Wilmking, M., Hallinger, M., Lantz, T., Blok, D., … Hik, D. S. (2011). Shrub expansion in tundra ecosystems: Dynamics, impacts and research priorities. *Environmental Research Letters*, *6*(045509), 1–15.
Nippert, J. B., Ocheltree, T. W., Orozco, G. L., Ratajczak, Z., Ling, B., & Skibbe, A. M. (2013). Evidence of physiological decoupling from grassland ecosystem drivers by an encroaching woody shrub. *PLoS ONE*, *8*(12), e81630.
Nowacki, G. J., & Abrams, M. D. (2008). The demise of fire and "mesophication" of forests in the eastern united states. *BioScience*, *58*(2), 123–17.
Petrie, M. D., & Brunsell, N. A. (2011). The role of precipitation variability on the ecohydrology of grasslands. *Ecohydrology*, *5*(3), 337–345.
Petrie, M. D., Brunsell, N. A., & Nippert, J. B. (2011). Climate change alters growing season flux dynamics in mesic grasslands. *Theoretical and Applied Climatology*, *107*(3-4), 427–440.
Porporato, A. (2003). Soil moisture and plant stress dynamics along the Kalahari precipitation gradient. *Journal of Geophysical Research*, *108*(D3), 4127. http://doi.org/10.1029/2002JD002448.
Ratajczak, Z., Nippert, J. B., Hartman, J. C., & Ocheltree, T. W. (2011). Positive feedbacks amplify rates of woody encroachment in mesic tallgrass prairie. *Ecosphere*, *2*(11), 1–14. https://doi.org/10.1890/ES11-00212.1
Ratajczak, Z., Nippert, J. B., & Ocheltree, T. W. (2014). Abrupt transition of mesic grassland to shrubland: Evidence for thresholds, alternative attractors, and regime shifts. *Ecology*, *95*(9), 2633–2645.

Ratajczak, Z., Nippert, J. B., Briggs, J. M., & Blair, J. M. (2014). Fire dynamics distinguish grasslands, shrublands and woodlands as alternative attractors in the Central Great Plains of North America. *Journal of Ecology*, *102*(6), 1374–1385.

Ratajczak, Z., Briggs, J. M., Goodin, D. G., Luo, L., Mohler, R. L., Nippert, J. B., & Obermeyer, B. (2016). Assessing the potential for transitions from tallgrass prairie to woodlands: Are we operating beyond critical fire thresholds? *Rangeland Ecology & Management*, *69*(4), 280–287.

Reichstein, M., Falge, E., Baldocchi, D., Papale, D., Aubinet, M., Berbigier, P., … Valentini, R. (2005). On the separation of net ecosystem exchange into assimilation and ecosystem respiration: Review and improved algorithm. *Global Change Biology*, *11*(9), 1424–1439.

Rosenstein, M. T., Collins, J. J., & De Luca, C. J. (1993). A practical method for calculating largest Lyapunov exponents from small data sets. *Physica D: Nonlinear Phenomena*, *65*(1-2), 117–134.

Sankaran, M., Hanan, N. P., Scholes, R. J., Ratnam, J., Augustine, D. J., Cade, B. S., … Zambatis, N. (2005). Determinants of woody cover in African savannas. *Nature*, *438*(7069), 846–849.

Schimel, D. S., Kittel, T. G. F., Knapp, A. K., Seastedt, T. R., Parton, W. J., & Brown, V. B. (1991). Physiological interactions along resource gradients in a tallgrass prairie. *Ecology*, *72*(2), 672–684.

Schlaepfer, D. R., Bradford, J. B., Lauenroth, W. K., Munson, S. M., Tietjen, B., Hall, S. A., … Jamiyansharav, K. (2017). Climate change reduces extent of temperate drylands and intensifies drought in deep soils. *Nature Communications*, *8*, 1–9. https://doi.org/10.1038/ncomms14196

Scholes, R. J., & Archer, S. R. (1997). Tree-grass interactions in savannas. *Annual Review of Ecology and Systematics*, *28*, 517–544.

Staver, A. C., Archibald, S., & Levin, S. A. (2011). The global extent and determinants of savanna and forest as alternative biome states. *Science*, *334*(6053), 230–232.

Stevens, N., Lehmann, C. E. R., Murphy, B. P., & Durigan, G. (2016). Savanna woody encroachment is widespread across three continents. *Global Change Biology*, *23*(1), 235–244.

Twidwell, D., Fuhlendorf, S. D., Taylor Jr., C. A., & Rogers, W. E. (2013). Refining thresholds in coupled fire-vegetation models to improve management of encroaching woody plants in grasslands. *Journal of Applied Ecology*, *50*(3), 603–613.

Twidwell, D., Rogers, W. E., Fuhlendorf, S. D., Wonkka, C. L., Engle, D. M., Weir, J. R., … Taylor Jr., C. A. (2013). The rising Great Plains fire campaign: Citizens' response to woody plant encroachment. *Frontiers in Ecology and the Environment*, *11*(s1), e64–e71.

Van Auken, O. W. (2000). Shrub invasions of North American semiarid grasslands. *Annual Review of Ecology and Systematics*, *31*, 197–215.

Walker, B. H., & Noy-Meir, I. (1982). Aspects of the stability and resilience of savanna ecosystems. In B. J. Huntley & B. H. Walker (Eds.), *Ecology of tropical savannas* (pp. 556–590). Berlin, Heidelberg: Springer.

Wonkka, C. L., Twidwell, D., West, J. B., & Rogers, W. E. (2016). Shrubland resilience varies across soil types: Implications for operationalizing resilience in ecological restoration. *Ecological Applications*, *26*(1), 128–145.

Xu, X., Medvigy, D., & Rodriguez-Iturbe, I. (2015). Relation between rainfall intensity and savanna tree abundance explained by water use strategies. *Proceedings of the National Academy of Sciences of the United States of America*, *112*(42), 12,992–12,996.

Ying, Z., Liao, J., Liu, Y., Wang, S., Lu, H., Ma, L., … Li, Z. (2017). Modelling tree-grass coexistence in water-limited ecosystems. *Ecological Modelling*, *360*, 387–398.